

University of Arkansas, Fayetteville

ScholarWorks@UARK

Biomedical Engineering Undergraduate Honors
Theses

Biomedical Engineering

5-2018

3D Printed Force Transducers for In-Vitro Mitral Valve Chordae Tendineae Force Measurements

Hayley Chandler

University of Arkansas, Fayetteville

Follow this and additional works at: <https://scholarworks.uark.edu/bmeguht>



Part of the [Biomechanics and Biotransport Commons](#), and the [Systems and Integrative Engineering Commons](#)

Citation

Chandler, H. (2018). 3D Printed Force Transducers for In-Vitro Mitral Valve Chordae Tendineae Force Measurements. *Biomedical Engineering Undergraduate Honors Theses* Retrieved from <https://scholarworks.uark.edu/bmeguht/62>

This Thesis is brought to you for free and open access by the Biomedical Engineering at ScholarWorks@UARK. It has been accepted for inclusion in Biomedical Engineering Undergraduate Honors Theses by an authorized administrator of ScholarWorks@UARK. For more information, please contact scholar@uark.edu, uarepos@uark.edu.

**3D Printed Force Transducers for In-Vitro Mitral Valve Chordae
Tendineae Force Measurements**

An Undergraduate Honors College Thesis

in the

Department of Biomedical Engineering

University of Arkansas

Fayetteville, AR

By

Hayley Chandler

April 27, 2018

Abstract

Mitral valve surgery is incredibly prevalent in the United States with more than 40,000 mitral valve surgical procedures annually. Improving the imaging techniques used to diagnose these cases requires validation of 3D models through experimental data such as mechanical properties of the tissue. An essential part of this process for the mitral valve is measuring the force experienced by chordae tendineae. This has been achieved with brass force transducers but using a 3D printed design can have many benefits. In this study, 3D printed miniature c-shaped force transducers comparable to previous metal models were designed and created using Solidworks 2016. Static force simulations were conducted in Solidworks and interpreted using Finite Element Analysis software within Solidworks. Forces typically experienced by the mitral valve (0.2N-1.5N) were applied and resultant strain was measured. The transducer frames experienced $83.23\mu\epsilon$ - $624\mu\epsilon$ on the inner face of c-shape and $55.4\mu\epsilon$ - $415.5\mu\epsilon$ on the outer face of the c-shape. This indicated a strain range of about 0.7% which is well within the range of the selected strain gauges for this application. The 3D printed design achieves similar strain range experienced at regions of strain gauge application and is faster and relatively easy to produce.

1. Introduction

The mitral valve is one of four valves located within the heart that are essential for proper cardiac function. This valve is positioned between the left atrium and ventricle and prevents backflow from the ventricle to the atrium (1). It is composed of an anterior and a posterior leaflet that come together to close the valve when the pressure in the left ventricle exceeds that of the left atrium (2). The leaflets are held onto by chordae tendineae, which are small fibrous chords that attach the leaflets to the papillary muscles (1). The chordae are necessary for the valve to function properly by preventing the leaflets from extending or bulging up into the left atrium when closed (3). Understanding the anatomy and physiology of the mitral valve is essential to prepare for surgical intervention.

The mitral valve is involved in more than 40,000 surgeries per year in the United States alone (4). Typically, repairing the mitral valve is preferred over replacing the valve and is one of the most commonly performed surgeries to treat mitral valve regurgitation (5). The choice to repair or replace is generally decided by the diagnosis of the patient, which is most often determined through 2D echocardiography. Echocardiography has drastically improved in the past few decades, but using 2D echocardiography can lead to overdiagnosis or can sometimes not adequately prepare the surgeon for intervention. To improve the imaging techniques used to diagnose problems with the mitral valve, physicians are turning to 3D rendering of patient valves (6). Although 3-dimensional images of the mitral valve are extremely beneficial, a computational model must be validated and given context with experimental data such as mechanical properties.

Mitral valve chordae tendineae force measurements have been obtained previously with force transducers typically made of metal (7,8,9). The more precise force measurements were obtained using c-shaped force transducers with a half bridge circuit utilizing two strain gauges on the inner and outer side of the c-shape. As the chordae tendineae begin to experience force, the ends of the c-shape are pulled away from each other, applying a compression force to the outer strain gauge and tensile force to the inner strain gauge (8).

Although these metal transducers were successful, a more precise and easy to produce material would be beneficial. Additive manufacturing (3D printing) has become increasingly popular as print quality increases and material properties diversify while also becoming less expensive (10). When considering force transducer applications, metals typically have higher strength, but will have lower density and will reach higher strains before failure (10). The possibility for higher strain rates can allow for more precise force calculations because the entire strain range of the strain gauges can be utilized and small differences in strain can be differentiated. Linear 3D printed miniature force transducers have shown to be capable of resolutions in the micronewtons range regardless of whether they were constructed using fused deposition molding or stereolithography 3D printing methods (11). This study aims to characterize the mechanical properties of the mitral valve by using c-shaped 3D printed force transducers to measure the force experienced by the chordae tendineae of the mitral valve.

2. Materials and Methods

2.1 Force Transducer Frame Design

Using the brass force transducers by Nielsen et al. for inspiration, miniature c-shaped force transducers were designed in Solidworks 2016 (Dassault Systemes, Vélizy-Villacoublay,

France). The determined frame design is essentially a thickened c-shape requiring three main structural features. A vertical rectangular slot is cut from the ends of the c-shape to allow for a chordae tendineae to be pressed into the frame. The chordae will be pre-loaded with a suture knot respective to the distance between the c-shape ends. This suture threads from the inside of the slot through a hole running transversely across the ends of the transducer frame. The suture then secures this chord against the slot by anchoring through a slit on the opposite side.

This structure was designed in Solidworks by creating concentric ovals of 4mm minor axis and 6mm major axis diameter for the inner oval and 6mm minor axis and 10mm major axis for the outer oval. A 90° region was removed from the c-shape on the right side by creating new endpoints with the line tool and removing the excess using the Trim Entities tool. This shape was then extruded 2mm to create the 3D basis of the transducer.

After the main shape was created, the structural features were added. To create the slots that house the chordae tendinae, a reference plane was generated at the top of the design and a rectangular shape of 0.5mm diameter was drawn and then extruded cut through the frame to allow the chord to lay flat against the transducer frame, minimizing the change to original chord geometry. Using this same method, the c-shape ends were also flattened to reduce overall size of the structure. The holes for suture threading were cut using a Ø1 dowel hole size with the Hole Wizard tool and positioned so that the holes overlapped with the slot for the chordae tendineae. This ensures that regardless of which side the chords are pre-sutured on, the suture can thread through the holes from the inside of the slot. Additionally, the slit for anchoring was also created by generating a reference plane tangent to the outer oval and using the Extruded

Cut feature. Finally, all edges of the design were filleted to minimize the risk of slicing the suture while mounting the chordae. The final design can be seen in Figure 1.

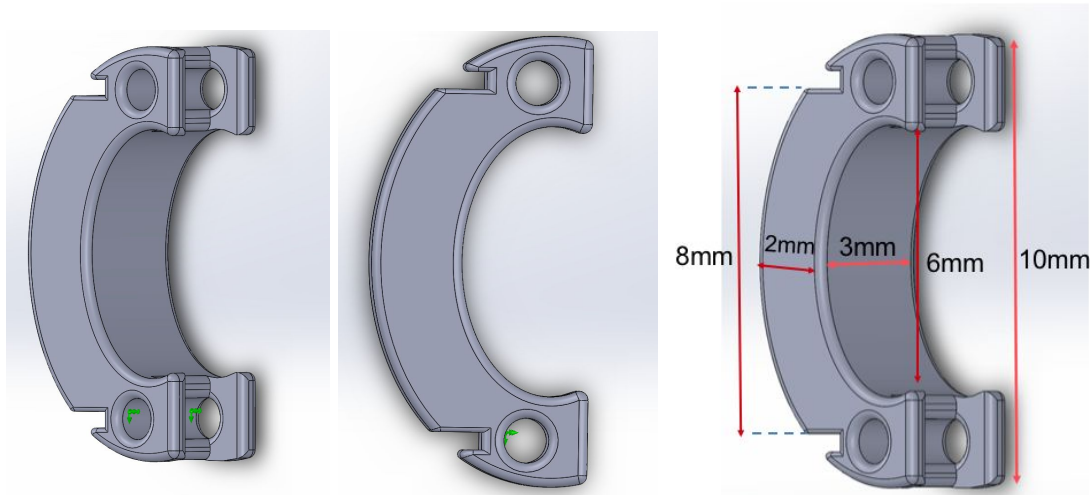


Figure 1. Final design of force transducer frame in Solidworks

2.2 Finite Element Analysis

To determine that the frame design was appropriate for force transducer applications, Finite Element Analysis simulations were performed in Solidworks. First, a Mesh Quality Analysis was conducted in Solidworks to confirm the accuracy of intended simulations. Mesh quality determines the accuracy of stress tests in Solidworks by dividing the structure into tetrahedral elements with as uniform geometry as possible. Two criteria can be used to quantify the accuracy of a mesh: aspect ratio and jacobian. The aspect ratio is defined as “the ratio between the longest distorted edge and the short normal dropped from a vertex to the opposite face normalized with respect to a perfect tetrahedral” (12). The Jacobian plot measures the deviation of an element created by the mesh from an ideally shaped tetrahedral element (13).

Solidworks simulation tools were used to determine the strain range experienced by the frame design in the regions of strain gauge placement. Material properties of both the FDP printing material (ABS) with the Makerbot printer and stereolithography printing material with the Objet (VeroWhite) were applied to the simulation and can be seen in Figure 2.

Property	Value	Units	Property	Value	Units
Elastic Modulus	2000	N/mm ²	Elastic Modulus	2500	N/mm ²
Poisson's Ratio	0.394	N/A	Poisson's Ratio	0.38	N/A
Shear Modulus	318.9	N/mm ²	Shear Modulus	1000	N/mm ²
Mass Density	1020	kg/m ³	Mass Density	1020	kg/m ³
Tensile Strength	30	N/mm ²	Tensile Strength	58	N/mm ²
Compressive Strength		N/mm ²	Compressive Strength		N/mm ²
Yield Strength		N/mm ²	Yield Strength	58	N/mm ²
Thermal Expansion Coefficient		/K	Thermal Expansion Coefficient		/K
Thermal Conductivity	0.2256	W/(m·K)	Thermal Conductivity	0.225	W/(m·K)

Figure 2. a) ABS material properties as defined by pre-set Solidworks values b) VeroWhite material properties defined by the manufacturer used to create a custom Solidworks material(14)

Simulations were set up by choosing regions of the design to remain fixed and applying desired forces in a selected direction. Because the mitral valve chordae tendineae typically experience between 0.2N-1.5N of force during normal valve function, simulations with increasing force in increments of 0.1N over this range were applied on the upper portion of the force transducer while the lower portion remained fixed (8). Detailed descriptions of fixed geometry and force applied can be seen in Figure 3.

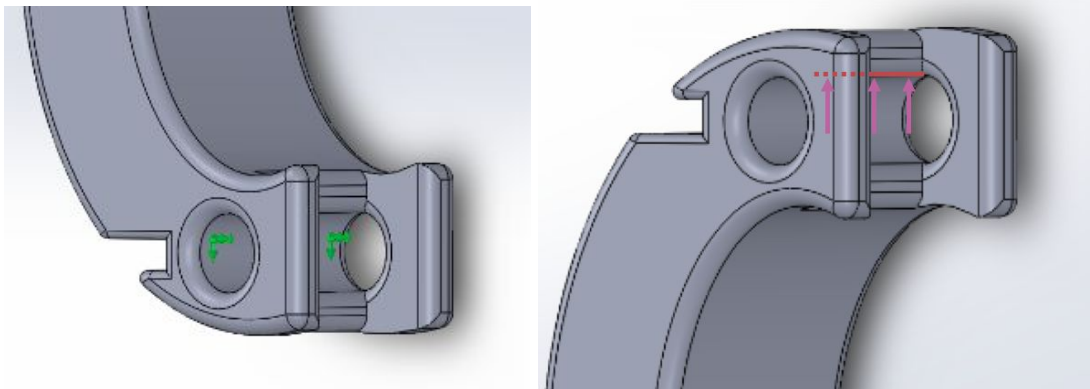


Figure 3. a) Locations of fixed geometry for simulation b) Locations of applied force toward reference plane tangent to top of transducer frame

2.3 Printing with Makerbot and Objet

A major design limitation of the force transducer design was the resolution of the available 3D printers and the small size necessary to reduce the effect on valve physiology. The Makerbot Replicator 2X has a resolution of about 100 microns, and a recommended minimum layer thickness of about 0.2mm (15). The Objet has a resolution of about 0.11 microns, with a minimum layer thickness of about 0.03mm. In addition, the Makerbot Replicator 2X is an extrusion based printer while the Objet uses Polyjet technology to cure thin layers of the printing material using UV energy (16).

2.4 Strain Gauge Selection and Mounting

There are several factors to consider when choosing a strain gauge for force transducer applications. Parameters such as the alloy used for the foil grid, backing material, temperature, resistance, and most importantly for miniature force transducers the gauge length. The selection process requires compromise between the best qualities of these factors to suit the needs of the

application for accuracy, environment, temperature, and duration of the test (17). The model strain gauge type follows the following formula for letter and number designation:

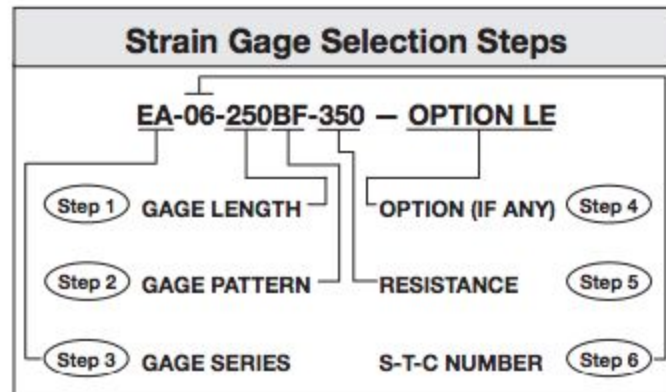


Figure 4. Strain Gauge Selection Steps and formula by Vishay Measurements Group (17)

The gauge series is determined by the chosen combination of backing material and foil grid. The backing material is important because it provides a means for handling during installation, provides the surface for adhesion, and also acts as insulation between the foil and transducer frame. Vishay Measurements Group provides two options for backing material: polyimide (E type) and glassfiber-reinforced epoxy-phenolic (W type). The E type polyimide backing material was chosen for this application because it is capable of large elongations and is easily contoured, which is essential to adhere to the c-shape design. The alloy used for the foil grid is strain-sensitive and is the major component in determining the characteristics of the strain gauge. The foil grid can be made out of Constantan (A type), Annealed constantan (P type), Isoelastic (D type), or Nickel-chromium (K type) alloy. Constantan was chosen for this application because of the high strain sensitivity and compatibility with small grid systems (17). The S-T-C number is the degree of self-temperature compensation and depends on the thermal expansion coefficient of the material used, and typically the 06 value is sufficient (18). In order to fit the size requirements of the transducer, a gauge length number of 031 corresponding to

0.032 inches (0.81mm) was necessary to fit on the inner and outer c-shape (19). The foil backing extends to 3mm but can be cut to within 0.1mm of the gauge matrix which may be slightly necessary for this design. The gauge pattern can be a single grid (DE type) or some form of a two- or three-element rosette. The force transducers will be experiencing uniaxial stress therefore only a single grid gauge pattern is necessary (17). As for resistance of the strain gauge, it is advised that the highest resistance available should be chosen to reduce heat dissipation. Based on other selected features, both 120 Ω and 350 Ω resistance were available, and a resistance of 350 Ω was chosen(17,19). These selections resulted in the Vishay model EA-06-031DE-350 model to be selected for this application which can be seen in Figure 5. This strain gauge has a strain range of $\pm 3\%$ and a temperature range of -100° to $+350^{\circ}$ (19). This was also the strain gauge model selected for use with the brass c-shaped force transducers design by Nielsen et. al (8).

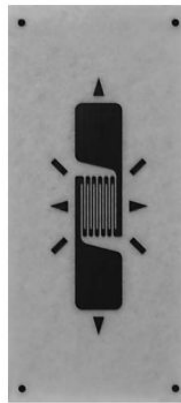


Figure 5. Vishay Measurements Group model EA-06-031DE-350 strain gauge

3. Results

3.1 Finite Element Analysis

A mesh was generated using the Solidworks Simulation tool and plots for Aspect Ratio and Jacobian were created and can be seen in Figure 6.

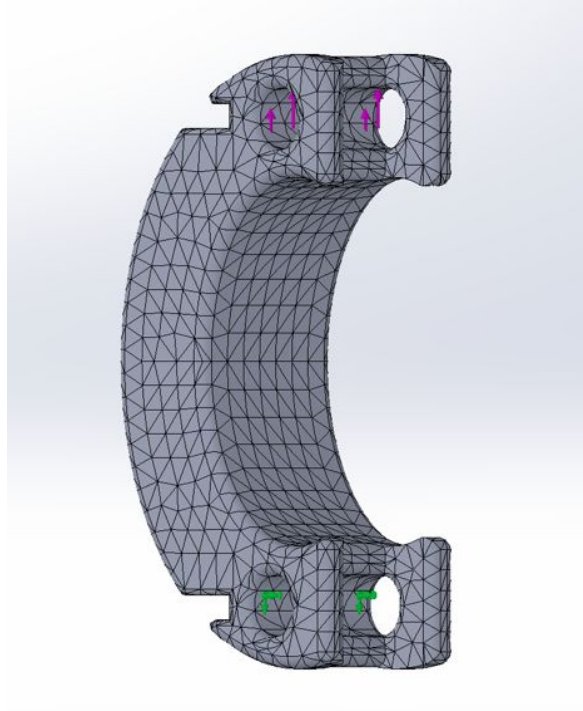


Figure 6. Mesh generated in Solidworks for the force transducer frame.

The mesh generated resulted in roughly 8 layers which indicates a “fine mesh” (12). Next, the aspect ratio and Jacobian plots were generated as seen in Figure 7.

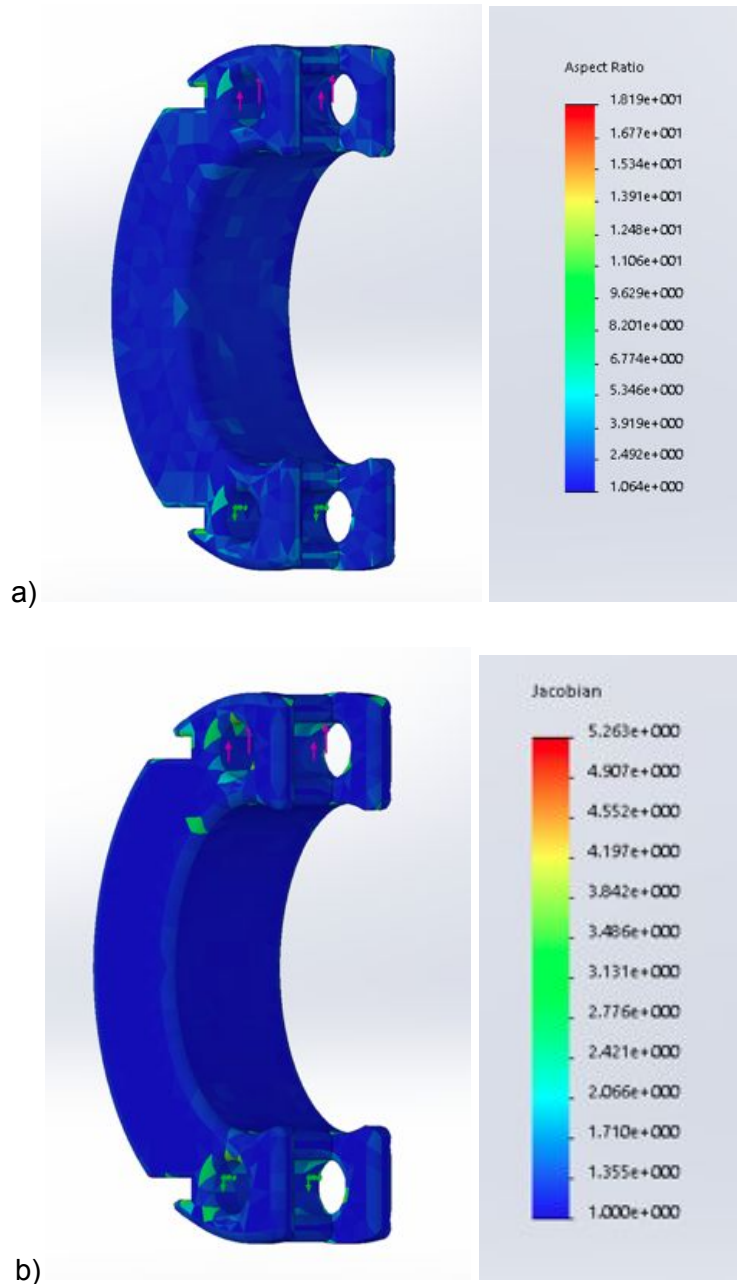


Figure 7. a) Aspect ratio plot of force transducer frame; b) Jacobian plot of force transducer frame

The majority of the mesh has an aspect ratio between 1.064 and 6.774, with a maximum aspect ratio of 18.19 at corners shown in Figure #. An ideal aspect ratio would be 1.0, however aspect ratios less than 40 are considered acceptable (12). The maximum aspect ratio generated by this

transducer frame design does not exceed twenty, which is half of the recommended maximum. When considering the Jacobian plot, calculations between 1.0 and 50 are considered acceptable (12). All values on the Jacobian plot were between 1.0 and 5.263. For both plots, the maximum and most undesirable values were located in positions not affecting the placement of the strain gauge as seen in Figure 8, therefore these results are not relevant. The results of both the Aspect Ratio check and Jacobian check indicate that further simulations of stress would be representative of the material used.

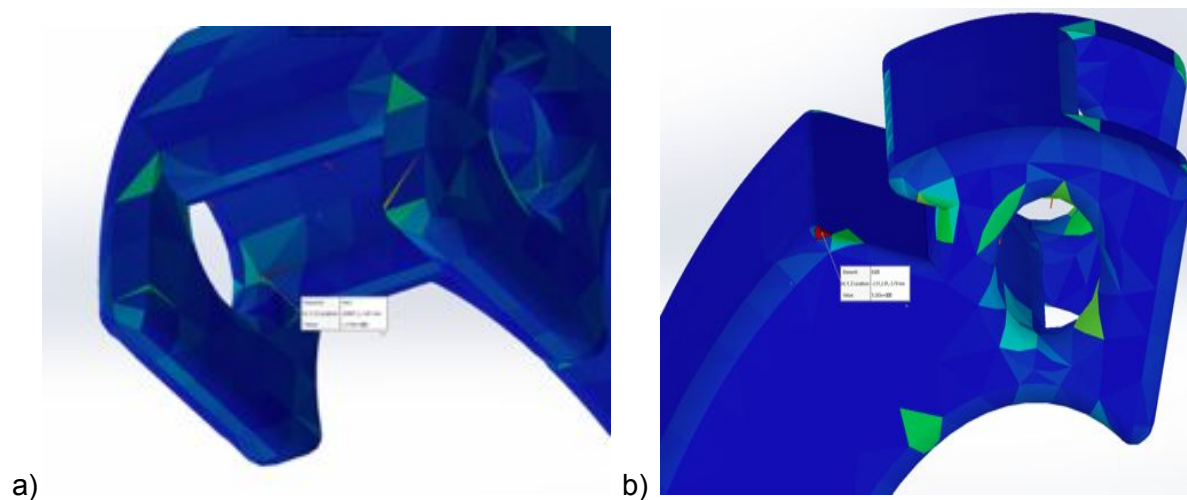


Figure 8. a) Point of maximum aspect ratio of 18.19; b) Point of maximum Jacobian of 5.263. Both values are well within the range of acceptable values, but are still irrelevant due to their position on the transducer frame

After the fixed geometry and regions of applied force were determined, varying force amounts were applied over the range of forces typically experienced by the chordae tendineae. The average strain of the inner c-shape and outer c-shape was calculated and can be seen in Table 1 and compared in Figure 9.

Table 1. Results of the applied force over typical valves experienced in vivo on both the inner c-shape and outer c-shape where the strain gauges will be applied.

Force Applied	Inner C-Shape Average Strain	Outer C-Shape Average Strain
0.2N	8.323E-05 (83.23 $\mu\epsilon$)	5.540E-05 (55.40 $\mu\epsilon$)
0.3N	1.248E-04 (124.8 $\mu\epsilon$)	8.310E-05 (83.10 $\mu\epsilon$)
0.4N	1.665E-04 (166.5 $\mu\epsilon$)	1.108E-04 (110.8 $\mu\epsilon$)
0.5N	2.081E-04 (208.1 $\mu\epsilon$)	1.385E-04 (138.5 $\mu\epsilon$)
0.6N	2.497E-04 (249.7 $\mu\epsilon$)	1.662E-04 (166.2 $\mu\epsilon$)
0.7N	2.913E-04 (291.3 $\mu\epsilon$)	1.939E-04 (193.9 $\mu\epsilon$)
0.8N	3.329E-04 (332.9 $\mu\epsilon$)	2.216E-04 (221.6 $\mu\epsilon$)
0.9N	3.745E-04 (374.5 $\mu\epsilon$)	2.493E-04 (249.3 $\mu\epsilon$)
1.0N	4.162E-04 (416.2 $\mu\epsilon$)	2.770E-04 (277.0 $\mu\epsilon$)
1.1N	4.578E-04 (457.8 $\mu\epsilon$)	3.047E-04 (304.7 $\mu\epsilon$)
1.2N	4.994E-04 (499.3 $\mu\epsilon$)	3.324E-04 (332.4 $\mu\epsilon$)
1.3N	5.410E-04 (541.0 $\mu\epsilon$)	3.601E-04 (360.1 $\mu\epsilon$)
1.4N	5.826E-04 (582.6 $\mu\epsilon$)	3.878E-04 (387.8 $\mu\epsilon$)
1.5N	6.242E-04 (624.2 $\mu\epsilon$)	4.155E-04 (415.5 $\mu\epsilon$)

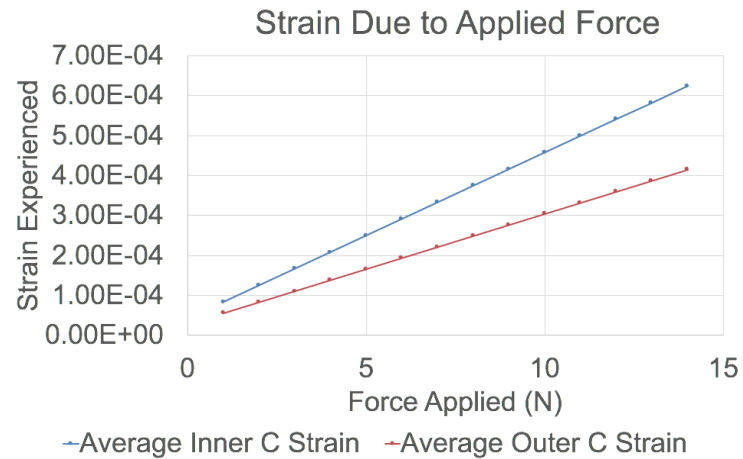


Figure 9. Comparison of strain experienced by inner and outer c-shape strange over the given force range

A separate simulation was also conducted in which an excessive force of 5N was applied to the transducer frame. This is about 3x higher than any stress that chordae tendineae would experience. The simulation results can be seen in Figure 10.

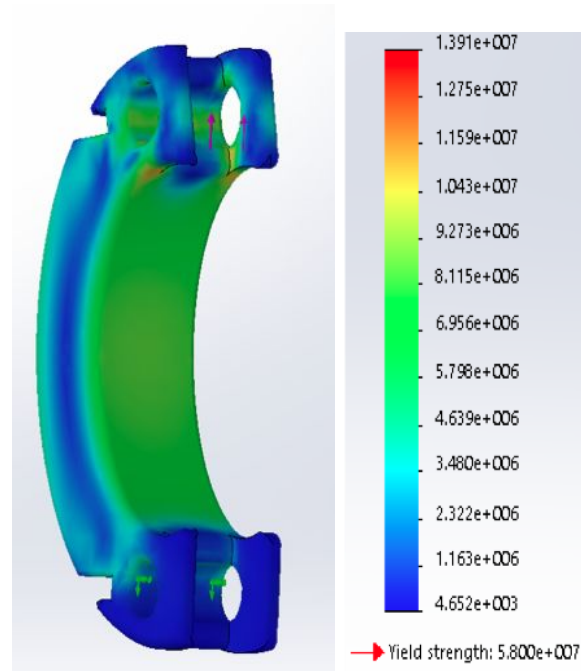


Figure 10. Results of Solidworks simulation of stress plot when applying 5N of static force to force transducers

Maximum stress values experienced did not exceed that of the yield stress of the material.

3.2 Printing with Makerbot and Objet

After running simulations, the force transducers were printed using the two 3D printers available in the Biomedical Engineering senior design lab. Due to the viscosity of the ABS material and larger layer thickness required, the Makerbot was unable to create sufficient prototypes for such a small and precise project. The layers of the transducer easily peeled apart and would not have been able to withstand the forces of the mitral valve. The resolution was also not accurate enough to create the necessary features such as the suture holes or anchor slit.

The Objet was much more successful at printing the force transducers with few errors. The duration of printing for three force transducer models was 60 minutes, with 15-30 minutes required to delicately remove the support material from the structure with a sewing needle. The printed prototype can be seen in Figure 11.

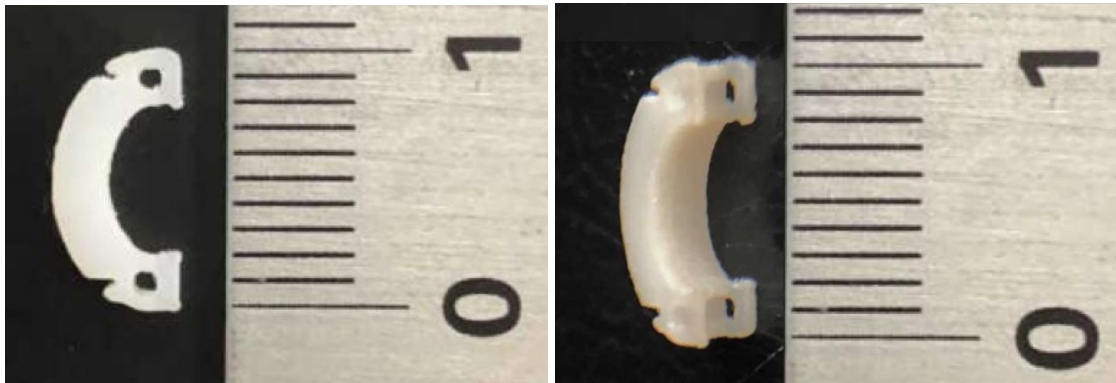


Figure 11. Results of 3D printing with VeroWhite material on Objet polyjet printer

4. Discussion and Future Work

Solidworks simulations of the transducer design show that 3D printed force transducers can achieve strain ranges appropriate for force transducer applications. It can be seen that the strain range for these force transducers is around 0.1% which is well within the $\pm 3\%$ range acceptable for the Vishay Model EA-06-031DE-350. The material properties indicate that the material could be elongated more than what was experienced in this simulation without failure. The 3D printing method used by the Objet resulted in accurate yet fragile structural features such as the anchoring slit. Removing the support material was a tedious process to ensure that the structural features were not disfigured. Reducing the transducer size with the Objet would be difficult, however, one possible area of improvement could involve thinning the c-shape from 3mm to a smaller width which may allow for a greater strain range to be experienced. This would potentially utilize the full range of the strain gauge and could better differentiate between small differences in strain.

Learning to mount the micro-measurements strain gauge to the frame and calibration was beyond the scope of this project. This will be completed by sending 3D printed prototypes of the transducer frames to Vishay Measurements Group in the UK to be mounted, calibrated and returned. The transducers will be ready to use when received from Vishay Measurements Group and will be used for future projects.

This design is part of a larger project system to measure force capabilities of the mitral valve chordae tendineae while mimicking physiological conditions. Once the strain gauges are mounted and calibrated, they will be attached to chordae tendineae of a porcine mitral valve sutured into a mitral valve holding apparatus designed at the University of Arkansas (20). This

holding apparatus fits into a left heart simulation tank designed by a senior design group in biomedical engineering. This tank allows for precise pressure control across the mitral valve, and will allow the force transducers to measure the force experienced by different mitral valve chordae tendineae types as the valve closes.

5. References

1. Kanjanauthai S, Sharma G. Mitral Valve Anatomy: Overview, Gross Anatomy, Microscopic Anatomy [Internet]. Emedicine.medscape.com. 2018 [cited 21 April 2018]. Available from: <https://emedicine.medscape.com/article/1878301-overview#a2>
2. Cardiac cycle - an overview | ScienceDirect Topics [Internet]. Sciencedirect.com. 2018 [cited 21 April 2018]. Available from: <https://www.sciencedirect.com/topics/neuroscience/cardiac-cycle>
3. Mestres, C.-A., & Bernal, J. M. (2012). Mitral Valve Repair: The Chordae Tendineae. *The Journal of Tehran University Heart Center*, 7(3), 92–99.
4. Mitral surgery
5. Mick, S. L., Keshavamurthy, S., & Gillinov, A. M. (2015). Mitral valve repair versus replacement. *Annals of Cardiothoracic Surgery*, 4(3), 230–237. <http://doi.org/10.3978/j.issn.2225-319X.2015.03.01>
6. Kamp D, Valocik G. Three-dimensional Echocardiography in Mitral Valve Disease. *European Cardiology Review*. 2005;;1.
7. He, Z. and Jowers, C. (2009). A Novel Method to Measure Mitral Valve Chordal Tension. *Journal of Biomechanical Engineering*, 131(1), p.014501.

8. Nielsen, S., Soerensen, D., Libergren, P., Yoganathan, A. and Nygaard, H. (2004). Miniature C-Shaped Transducers for Chordae Tendineae Force Measurements. *Annals of Biomedical Engineering*, 32(8), pp.1050-1057.
9. Jimenez, J., Soerensen, D., He, Z., Ritchie, J. and Yoganathan, A. (2005). Mitral Valve Function and Chordal Force Distribution Using a Flexible Annulus Model: An In Vitro Study. *Annals of Biomedical Engineering*, 33(5), pp.557-566.
10. Dizon, J., Espera, A., Chen, Q. and Advincula, R. (2018). Mechanical characterization of 3D-printed polymers. *Additive Manufacturing*, 20, pp.44-67.
11. J. Qu, Q. Wu, T. Clancy and X. Liu, "Design and calibration of 3D-printed micro force sensors," 2016 International Conference on Manipulation, Automation and Robotics at Small Scales (MARSS), Paris, 2016, pp. 1-4.
12. Mesh Quality Check: SOLIDWORKS Simulation (FEA) [Internet]. SEACAD. 2018 [cited 21 April 2018]. Available from:
<https://seacadtech.com/mesh-quality-check-solidworks-simulation-fea/>
13. Gokhale N. Practical finite element analysis. Pune: Finite To Infinite; 2008.
14. VeroWhite Plus POLYJET TECHNOLOGY MATERIAL SPECIFICATIONS [Internet]. Stratasysdirect.com. 2018 [cited 21 April 2018]. Available from:
https://www.stratasysdirect.com/wp-content/themes/stratasysdirect/files/material-datasheets/polyjet/PolyJet_VeroWhitePlus_Material_Specifications.pdf
15. Shop Replicator 2X Experimental 3D Printer | MakerBot [Internet]. Store.makerbot.com. 2018 [cited 21 April 2018]. Available from:
<https://store.makerbot.com/printers/replicator2x/>
16. Objet30 Pro | Stratasys [Internet]. Stratasys.com. 2018 [cited 21 April 2018]. Available from: <http://www.stratasys.com/3d-printers/objet30-pro>

17. Strain Gage Selection: Criteria, Procedures, Recommendations [Internet]. Vishaypg.com. 2018 [cited 21 April 2018]. Available from:
<http://www.vishaypg.com/docs/11055/tn505.pdf>
18. Stress Analysis Strain Gages [Internet]. Vishaypg.com. 2018 [cited 21 April 2018]. Available from:
<http://www.vishaypg.com/docs/11504/stress-analysis-selection-criteria.pdf>
19. Precision Strain Gages and Sensors [Internet]. Vishay Precision Group; 2018 [cited 21 April 2018]. Available from:
http://setpoint.gr/wp-content/uploads/micro-measurements_precision_strain_gages_catalog.pdf
20. Stephens S, Liachenko S, Ingels N, Wenk J, Jensen M. High resolution imaging of the mitral valve in the natural state with 7 Tesla MRI. PLOS ONE. 2017;12(8):e0184042.